ISSN 1063-7761, Journal of Experimental and Theoretical Physics, 2018, Vol. 126, No. 4, pp. 506–513. © Pleiades Publishing, Inc., 2018.
Original Russian Text © A.E. Petrova, A.I. Pankrats, 2018, published in Zhurnal Eksperimental'noi i Teoreticheskoi Fiziki, 2018, Vol. 153, No. 4, pp. 607–616.

ORDER, DISORDER, AND PHASE TRANSITION IN CONDENSED SYSTEM

Copper Metaborate CuB_2O_4 Phase Diagrams Based on the Results of Measuring the Magnetic Moment

A. E. Petrova[a,*] and A. I. Pankrats[b]

[a] *Institute for High Pressure Physics, Russian Academy of Sciences, Troitsk, Moscow, 108840 Russia*
[b] *Kirensky Institute of Physics, Krasnoyarsk Scientific Center, Siberian Branch, Russian Academy of Science, Krasnoyarsk, 660036 Russia*
**e-mail: apetrova@hppi.troitsk.ru*

Received October 22, 2017

Abstract—The magnetic phase transitions and the phase diagrams of the CuB_2O_4 multiferroic are studied. Phase diagrams of copper metaborate in a magnetic field directed along the [100] and [001] axes are plotted using the results of measuring the magnetic moment. Evidences for the existence of polycritical points are obtained.

DOI: 10.1134/S1063776118030172

1. INTRODUCTION

Deep interest in multiferroics is caused by the variety of magnetic and electric interactions in them, which result in the appearance of complex magnetic structures and diverse phase diagrams. This class of compounds includes the CuB_2O_4 copper metaborate, which solidifies in tetragonal noncentrosymmetric space group D_{2d}^{12} (which facilitates the formation of a chiral magnetic structure). This structure is characterized by nonequivalent sites of copper ions Cu(A) and Cu(B) [1–3]. Commensurate and incommensurate magnetic structures appear due to the interaction of two magnetic sublattices (Cu(A) and Cu(B)) [3, 4]. The existence of two magnetic sublattices and a noncentrosymmetric crystal structure cause the formation of complex magnetic structures and series of magnetic phase transitions. Such transitions were detected at low temperatures $T \approx 2$, 10, and 21 K in a zero magnetic field [5–7]. A phase transition from a paramagnetic state into a presumably long-period helicoidal structure takes place at $T \approx 20$ K [6]. When temperature decreases further to $T \approx 10$ K, the long-period helicoidal phase transforms into an incommensurate phase with a chiral magnetic structure and a spiral oriented along the [001] axis [2, 3]. The sequence of two first-order phase transitions at a temperature below 2 K is likely to correspond to transitions into a modulated state with wavevectors comparable with the lattice parameter [6]. Moreover, optical studies revealed two phase transitions in the incommensurate phase, namely, second-order transition at $T = 8.5$ K and first-order transition at $T = 8$ K, which is likely to cause an elliptical spin structure [8]. Using elastic neutron scattering, the authors of [7] detected two incommensurate phases in a magnetic field below 10 K, and a phase with a magnetic order corresponding to a soliton lattice forms in a magnetic field $H = 1.0$–1.5 T and a temperature below 4 K.

Although the contours of the CuB_2O_4 phase diagram in a magnetic field were plotted from the results of earlier studies, the boundaries of the phase transitions obtained by different methods in different works are often conflicting if we take into account the experimental errors and some contradictory results. The purpose of this work is to perform precision magnetic-moment investigations of the phase transitions in copper metaborate in the temperature range 2–300 K and magnetic fields up to 9 T.

2. EXPERIMENTAL

Single crystals were grown by the Kyropoulos technique from a B_2O_3–CuO–Li_2O–MoO_3 melt [9, 10]. The CuB_2O_4 phase diagram was studied in a magnetic field on single crystals oriented along axes [100] ($2.9 \times 2.5 \times 2.2$ mm^3), [001] ($2 \times 3 \times 2$ mm^3), and [110] ($4 \times 2 \times 1$ mm^3). The magnetic moment was measured with a PPMS Quantum Design vibrating-sample magnetometer in the temperature range 2–300 K and magnetic fields up to 9 T.

The magnetic fields in all experiments were generated by a superconducting magnet therefore, the relative error of determining the magnetic field turned out to be high because of a frozen magnetic field at its low values. The magnetic field in the cases where $H \approx 4 \times 10^{-4}$ T was indicated was calculated on the assumption that magnetic susceptibility χ in the paramagnetic temperature range was independent of a low magnetic

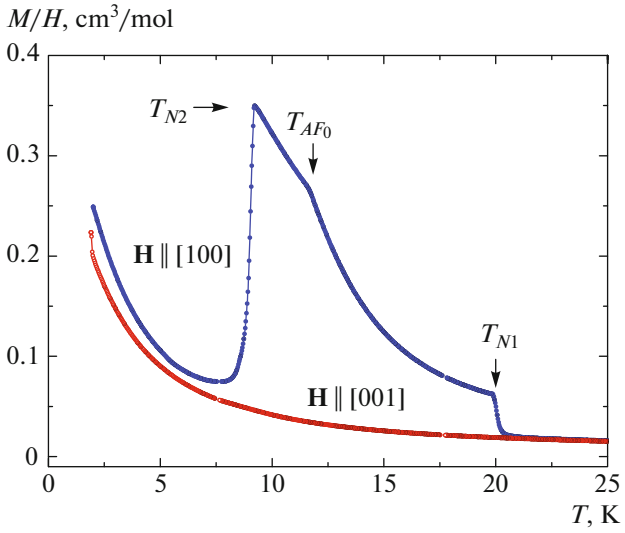

Fig. 1. (Color online) Temperature dependences of the magnetic susceptibility along the crystallographic [100] and [001] axes in a magnetic field of 0.03 T.

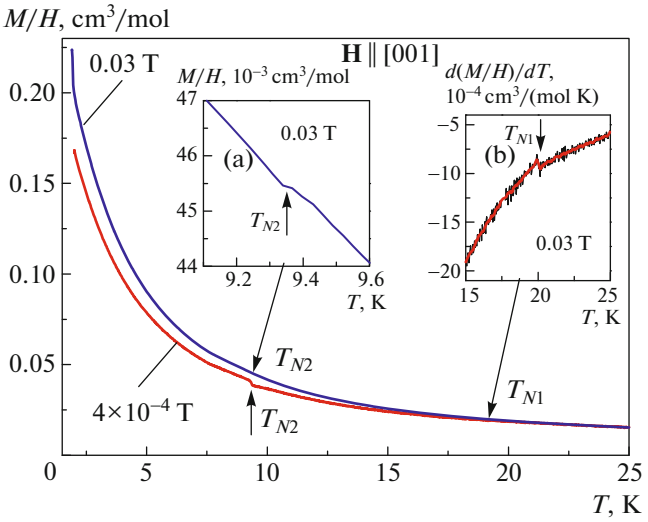

Fig. 2. (Color online) Temperature dependences of the magnetic susceptibility in low magnetic fields. A magnetic field is parallel to the tetragonal axis of the crystal.

field. The lattice parameters of CuB_2O_4 were measured using X-ray powder patterns. Their values ($a = 11.4919(5)$ Å, $c = 5.6224(4)$ Å) agree with the data in [1].

3. RESULTS

The following designations of magnetic phases are used here: PM stands for a paramagnetic phase; AF with indices, for modulated magnetic phases in the temperature range 9.4–20 K; and P with indices, incommensurate magnetic phases in the temperature range 2–9.4 K. The designations related to magnetic transformations along the tetragonal axis and indicated by superscript c.

Figure 1 shows the temperature dependences of the magnetic susceptibility along the [100] and [001] axes in a magnetic field of 0.03 T. On the whole, these results coincide with the data obtained in [5, 7, 11]. A clear anisotropy of the magnetic moment is seen when a magnetic field is oriented along and across the tetragonal axis. At first glance, the magnetic susceptibility along the tetragonal axis increases monotonically according to the Curie–Weiss law when temperature decreases and deviates slightly from this law at low temperatures. However, under close examination, the following weak signs of phase transformations are visible: a magnetic susceptibility jump from an incommensurate phase to a modulated one at $T_{N2} = 9.4$ K in a magnetic field $H \approx 4 \times 10^{-4}$ T (Fig. 2) and a jump of the derivative at the point of phase transition from an ordered state into a paramagnetic one at $T_{N1} = 20$ K (Fig. 2b). In addition, the jumplike behavior degenerates at T_{N2} when the magnetic field increases to 0.03 T (Fig. 2, inset a).

An analogous situation is observed in the magnetic field directed along [100]: the signs of a phase transition change radically when the magnetic field increases slightly. Figure 3 shows the temperature dependence of the magnetic susceptibility in magnetic fields $H \approx 4 \times 10^{-4}$ T and $H = 0.03$ T. It is seen that, when the incommensurate phase transforms into the modulated phase at T_{N2}, function $\chi(T)$, which tends toward infinity at the point of transition in a field $H \approx 4 \times 10^{-4}$ T, degenerates into a finite jump at a relatively low field of 0.03 T. The less pronounced magnetic susceptibility peak for the transition of the modulated phase into the paramagnetic state at T_{N1} changes into an almost simple step at 0.03 T (inset to Fig. 3). Here, work [12] is worth noting: the magnetic moments measured in that work differ radically from the results of our measurements and the data obtained in [5, 11]. This difference is likely to be related to the error in crystal orientation and incorrect magnetic susceptibility calculations.

We now consider the field dependences of the magnetic moment at low temperatures. Figure 4 shows the saturation of the magnetic moment at a temperature of 2 K. A weak anisotropy of magnetic moment saturation is observed in the magnetic fields directed along and across the tetragonal axis. A phase transition occurs near the saturation region in field H_{P2}, and it is accompanied by a pronounced magnetic moment jump in the magnetic field along [100]. However, the magnetic moment jump in the magnetic field directed along the tetragonal axis is weak and takes place in significantly higher magnetic field H^c_{P3} almost in the magnetic moment saturation region. The effective magnetic moments determined from the high-tem-

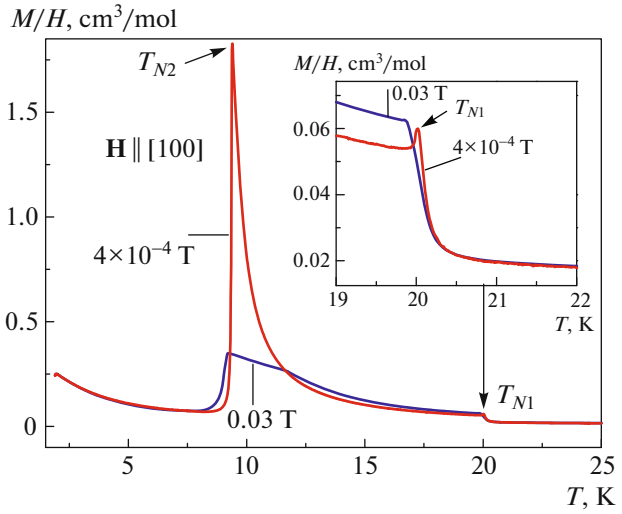

Fig. 3. (Color online) Temperature dependences of the magnetic susceptibility in low magnetic fields. A magnetic field is parallel to [100].

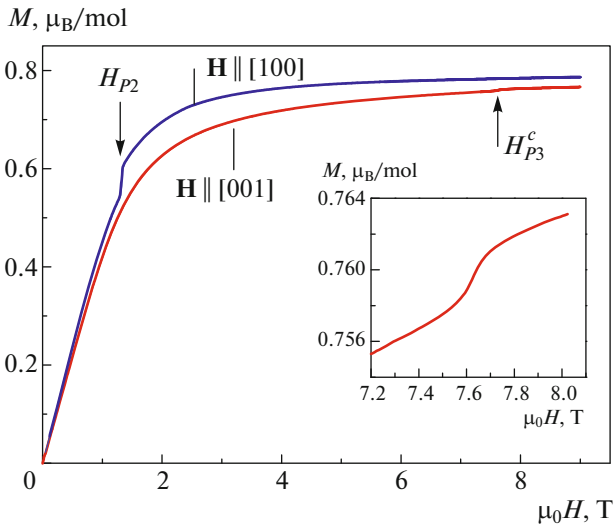

Fig. 4. (Color online) Field dependences of the magnetic moment at 2 K. A magnetic field is parallel and perpendicular to the tetragonal axis of the crystal.

perature part of the magnetic susceptibility in the [001] and [100] directions are $\mu_{eff} = 1.86\mu_B$ and $1.83\mu_B$, respectively. On the whole, these values are close to the value ($\mu_{eff} = 1.77\mu_B$) obtained in [13]. The insignificant difference is likely to be related to the error of determining the magnetic field and the different sample geometries. The saturation magnetic moment is estimated at $\mu_s \approx 0.79\mu_B$. Thus, the spin estimated from the effective magnetic moment without regard for the orbital moment is 0.54, which is close to the spin for Cu^{2+} ($S = 1/2$); the value estimated from the saturation magnetic moment is slightly underestimated. A rough linear-approximation estimation yields about 100 T for the magnetic field at which the magnetic moment can be saturated.

We now consider the behavior of the magnetic properties in high magnetic fields. Figures 5 and 6 show the temperature dependences of the magnetic susceptibility for dc magnetic fields directed along and across the tetragonal axis.[1] As is seen in Figs. 5 and 6, the behavior of magnetic susceptibility actually reflects an almost linear character of the magnetic moment (at a constant temperature) at relatively high temperatures in low magnetic fields. At a temperature below 10 K, the magnetic moment tends toward saturation at $H = 3$ T (Fig. 5). The surprising thing is that the changes in the magnetic susceptibility that indicate a phase transition from the incommensurate phase into the modulated one at T_{N2}, which are poorly pronounced in low fields, change insignificantly in amplitude in the region of transition into an induced ferromagnet (Fig. 5a). Therefore, we can trace the field dependence of critical temperature T_{N2} up to the saturation field. Note that the point of transition from a weakly ferromagnetic phase into a paramagnetic state (T_{N1}) cannot be detected in fields higher than 5 T at the existing experimental error. This feature is likely to be caused by the fact that, when the magnetic field increases, the boundary between the paramagnetic and weakly ferromagnetic phases smears because of gradual transition of the paramagnetic phase into the induced ferromagnetic phase.

The evolution of the phase transitions with the magnetic field directed along [100] can be traced in Fig. 6. As would be expected (see Figs. 1, 3, 4), the transitions from the incommensurate into the modulated phase at T_{N2} and from the modulated into the paraphase at $T = T_{N1}$ are accompanied by well-pronounced anomalies, which degrade with increasing magnetic field (Fig. 6). The magnetic susceptibility jump at T_{N1} at the boundary between the paramagnetic and modulated phases smears when the magnetic field increases. The sharp anomaly at $T = T_{N2}$, which is related to the transition between the modulated and incommensurate phases, shifts toward low temperatures and decreases in amplitude.

We now dwell on the sections of the magnetic susceptibility along the curves at a dc magnetic field and a constant temperature in a magnetic field directed along [100] (Fig. 7). The phase transition in the magnetic field range 0.3–1.25 T (Fig. 7a) and the temperature range 4.85–5.5 K (Fig. 7c) splits into two transitions, one of which exhibits pronounced temperature (Fig. 7b) and magnetic field hystereses. Obviously, these features are signs of a classical first-order phase

[1] Magnetic susceptibility is shown in most figures, since the change in the magnetic moments at a significant difference between the magnetic fields cannot be used to clearly trace the dynamics of phase transitions.

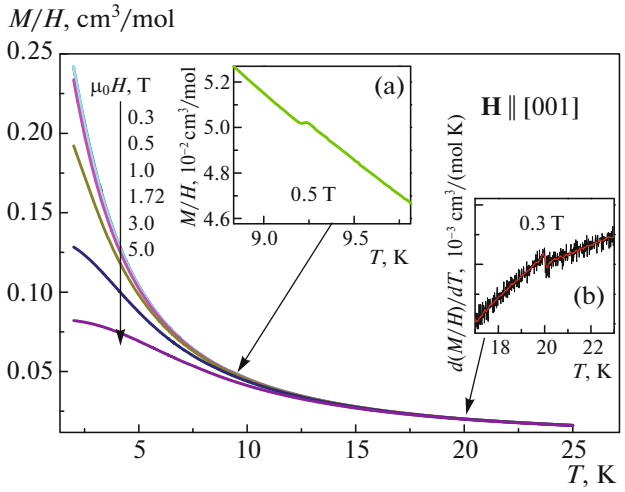

Fig. 5. (Color online) Temperature dependences of the magnetic susceptibility of a CuB_2O_4 single crystal for a magnetic field $\mu_0 H$ = 0.3, 0.5, 1.0, 1.72, 3.0, and 5.0 T applied along the tetragonal axis of the crystal.

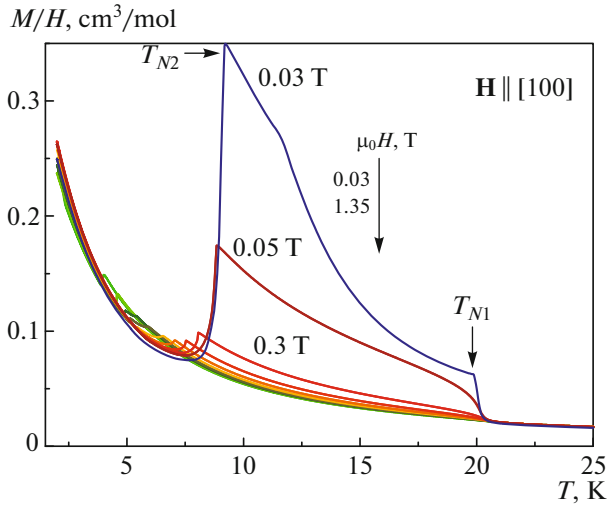

Fig. 6. (Color online) Temperature dependences of the magnetic susceptibility of a CuB_2O_4 single crystal for a magnetic field $\mu_0 H$ = 0.03, 0.08, 0.3, 0.5, 0.7, 0.88, 1.05, 1.15, 1.25, and 1.35 T applied along [100].

transition; the lower the amplitude of changing the magnetic susceptibility, the higher the hysteresis.

Taking into account the significant change in the magnetic susceptibility in low magnetic fields (see Figs. 2, 3), we focus on the magnetic field range $H <$ 0.5 T. Figures 8 and 9 show the behavior of the magnetic susceptibility in the modulated and incommensurate phases. Figure 10 depicts the initial segments of the field dependences measured at T = 10 K for fields directed along [100] and [110] and at T = 13 K for the [100] direction. As is seen from Figs. 8a and 8b, two singular points (H^c_{P1}, H^c_{P2}) in the incommensurate phase and one singular point ($H^c_{AF_0}$) in the modulated phase (Fig. 8c) can be detected in low magnetic fields directed along [001]. A similar picture is observed in a magnetic field directed along [100]: two well-pronounced features ($H^*_{AF_0}$, H_{AF_0}) exist in the temperature range 10–20 K at lower magnetic fields (Fig. 9b). At temperatures below the phase transition into the incommensurate phase, only one peak (H_{P0}) is clearly visible (apart from the peak corresponding to the AF_1–P_1 phase transition), which almost disappears at a temperature below 8 K (Fig. 9a). The absence of the low-temperature doublet in the [100] direction is assumed to be associated with a very low field and to be inside the measurement error; of course, this fact does not exclude the possibility of a single phase transition in a narrow temperature range.

4. COPPER METABORATE PHASE DIAGRAMS. DISCUSSION

The experimental results are presented in phase diagrams. Figures 11 and 12 display proposed copper metaborate phase diagrams in the temperature range 2–25 K and magnetic fields up to 9 T. Detailed investigations of these phase diagrams in comparison with the phase diagrams constructed in a magnetic field in [6, 14, 15] demonstrate that copper metaborate undergoes the magnetic phase transitions that have not been revealed in earlier experiments. Let us consider the results obtained in detail.

Based on the results of studying a magnetic resonance spectrum [6], we assume that a helicoidal long-period magnetic state exists in the temperature range T_{N1}–T_{N2} in the absence of a magnetic field. This assumption is indirectly supported by the magnetic susceptibility peak in an almost zero field (inset to Fig. 3). The magnetic moment of Cu(B) ions in the commensurate phase is directed along the tetragonal axis, and Cu(A) ions form an antiferromagnetic network in the basal plane [3]. The phase transition at T = 20 K in a magnetic field $H \approx 4 \times 10^{-4}$ T directed along [100] is accompanied by a small magnetic susceptibility peak (inset to Fig. 3). In the case $H \parallel$ [001], a phase transition is indicated by a very low derivative jump at temperature T_{N1} (see Fig. 2b).

The weakly ferromagnetic state in the temperature range T_{N1}–T_{N2} in a magnetic field directed along [100] is induced and appears in the magnetic field that exceeds a certain critical field H_{AF_0}. The magnetic structure of copper metaborate in a magnetic field lower than H_{AF_0} is assumed to be modulated, which leads to the absence of a spontaneous magnetic moment [6]. In this state, the field dependences of magnetization in the [100] and [110] directions are different in low fields. The initial segments of the field dependences measured at T = 10 K in magnetic fields

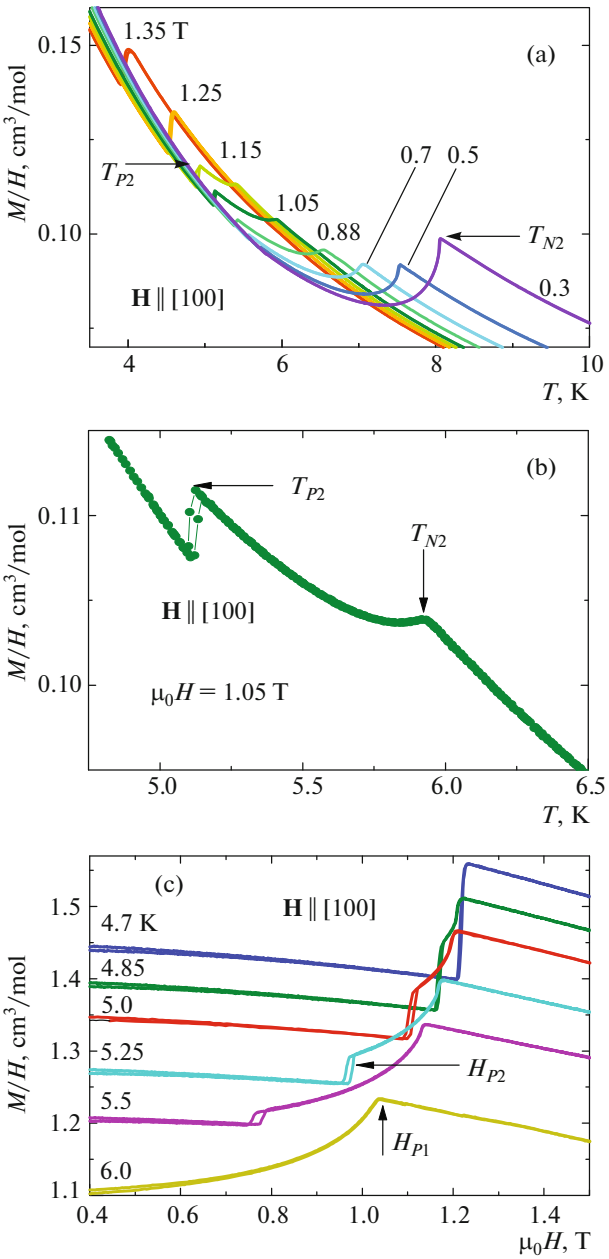

Fig. 7. (Color online) Temperature dependences of M/H in a magnetic field ($\mu_0 H$ = (a) 0.3, 0.5, 0.7, 0.88, 1.05, 1.15, 1.25, and 1.35 T and (b) 1.05 T and (c) field dependence of M/H at a constant temperature. a magnetic field is directed along [100].

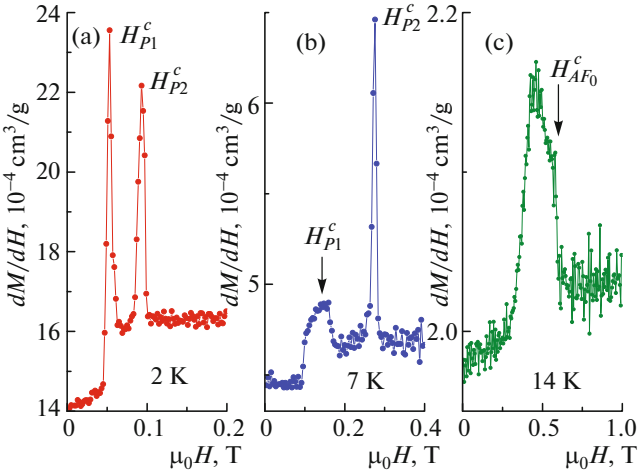

Fig. 8. (Color online) Differential magnetic susceptibility vs. magnetic field directed along [001] at a temperature of (a) 2, (b) 7, and (c) 14 K.

directed along axes [100] and [110] are shown in Fig. 10. Curve *1* in the [110] direction is smooth without inflection points, and field dependence of magnetization *2* in the [100] direction first lies below the dependence for [110] and then coincides with it beginning from field $H = H^*_{AF_0}$. For the [100] direction, the differential susceptibility in field $H^*_{AF_0}$ changes jumpwise. The difference in the field dependences is related to the magnetic anisotropy in the basal plane of CuB_2O_4.

Using $FeGe_2$ as an example, the authors of [16] theoretically and experimentally showed that the magnetic moment of an easy-plane tetragonal antiferromagnet magnetized in an easy direction in the basal plane increases linearly with the field and a spin-reorientation transition in the basal plane takes place when a field is oriented in the hard direction located at an angle of $\pi/4$ to the easy direction. Therefore, the [110] direction in the basal plane of CuB_2O_4 is an easy one, and field $H^*_{AF_0}$ is spin-reorientation field in which the rotation of magnetic moments from the [110] easy direction to the [100] hard direction ends. It also follows from the neutron data [3] that the [110] direction is an easy direction in the basal plane. Unlike the collinear $FeGe_2$ compound, the field dependences in the easy ([110]) and hard ([100]) directions in CuB_2O_4 are nonlinear up to field H_{AF_0}. This specific feature is most likely to be due to a modulated character of the structure in this state. In a magnetic field, the modulated structure transforms into a fan structure, and the behavior of magnetization depends on the direction (one of the two directions) in which a fan structure forms because of tetragonal in-plane anisotropy.

A magnetic hysteresis is observed at $H < H^*_{AF_0}$ during the forward and reverse motion of a magnetic field (Fig. 10, T = 13 K), which points to the fact that the reorientation is a first-order phase transition. An additional phase boundary caused by spin reorientation in the basal plane appears during magnetization in the basal plane in the [100] hard direction in low fields. The reorientation generates a differential susceptibility peak in a magnetic field of 0.016 T at a temperature of 14 K (see Fig. 9b). As the temperature

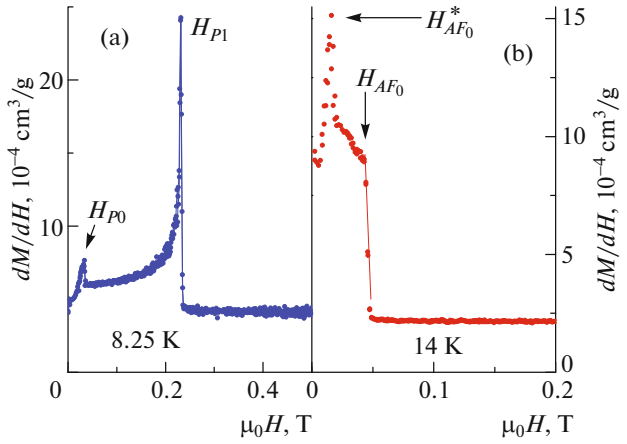

Fig. 9. (Color online) Differential magnetic susceptibility vs. magnetic field directed along [100] at a temperature of (a) 8.25 and (b) 14 K.

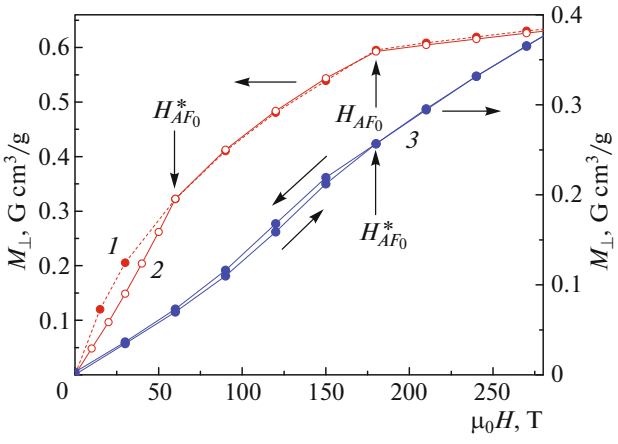

Fig. 10. (Color online) Field dependences of the magnetic moment: (*1*) $T = 10$ K, $\mathbf{H} \parallel [110]$; (*2*) $T = 10$ K, $\mathbf{H} \parallel [100]$; and (*3*) $T = 13$ K, $\mathbf{H} \parallel [100]$.

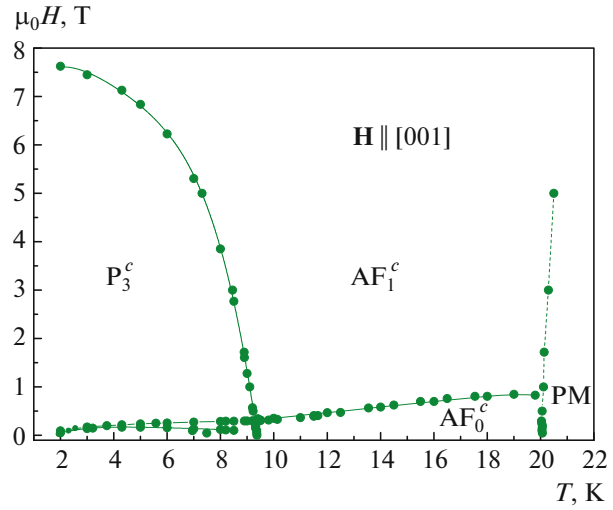

Fig. 11. (Color online) Magnetic phase diagram of copper metaborate CuB_2O_4. A magnetic field is directed along [001].

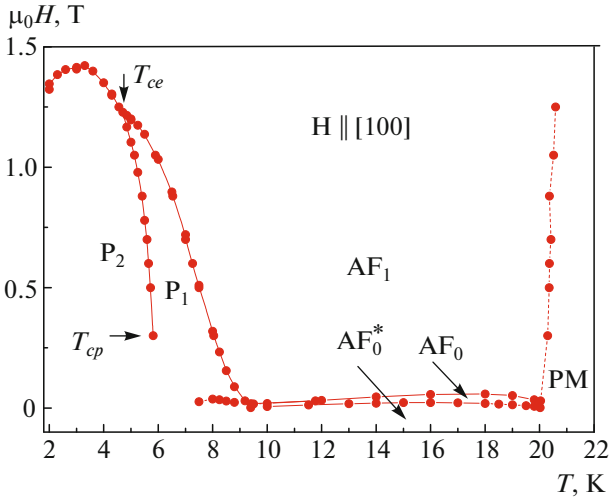

Fig. 12. (Color online) Magnetic phase diagram of copper metaborate CuB_2O_4. A magnetic field is directed along [100].

increases, spin-reorientation field $H^*_{AF_0}$ increases, reaches a maximum at 16 K, and begins to decrease when the Néel temperature is approached (Fig. 13a). The critical field of the AF_0–AF_1 phase transition into an induced weakly ferromagnetic state has a similar temperature dependence (Fig. 13a). The boundaries of the AF_0 and AF_1 phases are plotted using the characteristic points shown in Figs. 1 (T_{AF_0}) and 9b (H_{AF_0}).

When the temperature decreases further, a phase transition into another magnetic structure occurs; according to [3], this structure is incommensurate and the magnetic phase diagram becomes significantly complicated. Figure 13b shows a fragment of the phase diagram in a magnetic field up to 0.4 T directed along [001] for the temperature range 2–10 K. At least two different magnetic states bounded by lines P^{c_1} and P^{c_2} exist in low magnetic fields. Two clear differential susceptibility peaks in a magnetic field (H^c_{P1}, H^c_{P2}) are visible (see Figs. 8a, 8b). This behavior can be interpreted as spin reorientation in the B subsystem. In the absence of a magnetic field, the B subsystem has an antiferromagnetic component along the tetragonal axis, which can cause a magnetic transition [3].

Thus, the antiferromagnetic vectors of the B subsystem form a cone in the spiral state in low fields. We assume that a magnetic transition takes place in the range of fields H_{P1}–H_{P2} directed along [001], and the cone of antiferromagnetic vectors straightens gradu-

ally and transforms into a planar spiral lying in the basal plane. Only one magnetic transition and solely in the temperature range 7.5–8.8 K was detected in a low magnetic field directed along [100] in the temperature range 2–9.4 K (see Fig. 9a (H_{P0}) and 12). It is not clear whether this transition is related to the phase with an elliptical spin structure discovered recently [8]. We can only note that phase P_0 exists in a close temperature range.

We now consider the phase transition from the commensurate to the incommensurate phase. This phase transition is accompanied by a weak smeared jump in a magnetic field applied along the tetragonal axis (see Fig. 2a, inset to Fig. 4). The corresponding phase boundary separates phases AF_1^c and P_3^c in the phase diagram shown in Fig. 11. The AF_1^c–P_3^c phase transition is accompanied by a jump of transverse magnetization with a hysteresis [17] and a magnetostriction jump [15], which unambiguously points to a first-order phase transition. The transverse magnetization jump is close to the weakly ferromagnetic moment in the basal plane [17]. This finding proves the existence of a transition into an induced weakly ferromagnetic state when the critical field is achieved at a temperature below T_{N2}. The AF_1^c–P_3^c phase transition for a magnetic field oriented along the tetragonal axis is related to the fact that the spiral magnetic state is a collective magnetic state of copper metaborate, which is formed by both subsystems of copper ions. Magnetization along the tetragonal axis at low temperatures saturates the weak B subsystem and arranges it along the field direction. The spiral state exists until the transverse components of the magnetic moments of this subsystem are nonzero [4]. The longitudinal magnetization jump is associated with the weak subsystem, which is explained by the fact that the transverse components of the magnetization of the B subsystem vanish during the jump transition. As a result, a small longitudinal magnetization jump appears along the tetragonal axis and the spiral state is destroyed.

The situation in a magnetic field applied along [100] is slightly different. The AF_1–P_1 phase transition is likely to correspond to a second-order phase transition and determines the boundary between the commensurate and incommensurate phases in a magnetic field (see Fig. 7; T_{N2}, H_{P1}). When the magnetic field increases along [100], the phase transition splits suddenly into two transitions and a new phase (P_2) appears (see Fig. 7). Of course, the P_1–P_2 phase transition (see Fig. 12) is a first-order phase transition with a noticeable hysteresis (see Fig. 7; H_{P2}, T_{P2}). As follows from the behavior of the magnetic moment (Fig. 4, H_{P2}), the magnetic transition into the P_2 phase has the signs of a spin-flop transition (see Fig. 12). The phase transition with the P_1–P_2 and AF_1–P_2 boundaries is

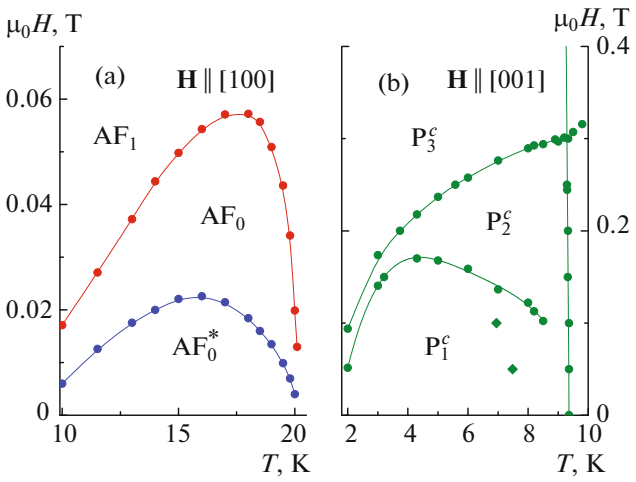

Fig. 13. (Color online) Phase diagrams (a) in the temperature range 10–20 K, $\mu_0 H < 0.07$ T, $\mathbf{H} \parallel [110]$ and (b) in the temperature range 2–10 K, $\mu_0 H < 0.4$ T, $\mathbf{H} \parallel [001]$.

assumed to be a spin-flop transition related to a weak anisotropy in the basal plane (see Fig. 12). As is seen from the phase diagram in Fig. 12, the second-order phase transition AF_1–P_1 line ends in the first-order spin-flop transition line at point T_{ce}, which is most likely to be an end critical point.

Another specific feature clearly visible in Fig. 12 is noteworthy. The P_1–P_2 phase transition line corresponding to the [100] magnetic field direction seems to terminates at point T_{cp} with coordinates 5.8 K and 0.3 T. A first-order phase transition cannot end simply; therefore, a critical or polycritical phenomenon is thought to take place here. It should be noted that we failed to experimentally detect signs of any transformations in magnetic fields at $T < 0.3$ T near T_{cp} within the limits of experimental error. Obviously, it is necessary to perform detailed investigations of the behavior of thermodynamic parameters, at least heat capacity and thermal expansion, in the vicinity of points T_{ce} and T_{cp}.

Let us generalize the aforesaid. The evolution of the magnetic susceptibility anomalies in the incommensurate phase allows us to state that end critical point T_{ce}, at which the line of a continuous phase transition intersects with the first-order phase transition line, exists at a temperature $T \approx 4.7$ K in a magnetic field $H \approx 1.2$ T directed along [100] [18]. The orientational magnetic P_1–P_2 spin-flop phase transition is accompanied by temperature and magnetic-field hystereses and is a first-order phase transition. The P_1–P_2 phase transition line ends at point T_{cp}, which is likely to be a critical point. The phase transition from the incommensurate to the commensurate phase in a magnetic field directed along [001] is a first-order phase transition [15, 17]. The magnetic transitions in

low magnetic fields are most likely to be first-order phase transitions.

On the whole, the phase diagrams presented in this work agree with the results from [5–7]. Magnetic phases, which have not been revealed earlier and lead to at least one polycritical point, were detected in a magnetic field in the temperature range 2–10 K. Note that we failed to reveal obvious signs of the phase transitions at 8.5 and 8 K in the incommensurate phase, which were found by optical methods in [8], and the soliton lattice "pocket" in a magnetic field $H \approx 1$–1.5 T at a temperature below 4 K [7].

5. CONCLUSIONS

Magnetic phase diagrams of copper metaborate CuB_2O_4 were plotted using the results of measuring the magnetic moment in the temperature range 2–300 K and magnetic fields up to 9 T. New magnetic phase states were detected in the temperature range 2–9.4 T, and additional, first of all, neutron diffraction studies are necessary to reveal the nature of these states. The behavior of the magnetic susceptibility anomalies in the incommensurate phase allows us to state that an end critical point exists in a phase diagram in a magnetic field applied along [100] at a temperature $T \approx 4.7$ K and a magnetic field $H \approx 1.2$ T and, apparently, a critical point exists at $T \approx 5.8$ K and $H \approx 0.3$ T. The orientational spin-flop transition into the P_2 phase is accompanied by temperature and magnetic-field hystereses and is a first-order phase transition. The magnetic transitions in low magnetic fields are most likely to be first-order phase transitions.

ACKNOWLEDGMENTS

We thank I.P. Zibrov for the lattice parameter measurements, K.N. Boldyrev for turning our attention to this topic and sharing the available samples, S.S. Khasanov for preparing the oriented samples, and S.M. Stishov for his support and many valuable discussions.

This work was supported in part by the Russian Foundation for Basic Research (project no. 18-02-00183-a) and the program "Condensed Matter Physics and New-Generation Materials" of the Presidium of the Russian Academy of Sciences.

REFERENCES

1. M. Martinez-Ripoll, S. Martinez-Carrera, and S. Garcia-Blanco, Acta Crystallogr. B **27**, 677 (1971).
2. B. Roessli, J. Schefer, G. A. Petrakovskii, B. Ouladdiaf, M. Boehm, U. Staub, A. Vorotinov, and L. Bezmaternikh, Phys. Rev. Lett. **86**, 1885 (2001).
3. M. Boehm, B. Roessli, J. Schefer, A. S. Wills, B. Ouladdiaf, E. Lelièvre-Berna, U. Staub, and G. A. Petrakovskii, Phys. Rev. B **68**, 024405 (2003).
4. S. N. Martynov and A. D. Balaev, JETP Lett. **85**, 649 (2007).
5. G. A. Petrakovskii, D. Velikanov, A. Vorotinaov, A. Balaev, K. Sablina, A. Amato, B. Roessli, J. Schefer, and U. Staub, J. Magn. Magn. Mater. **205**, 105 (1999).
6. A. I. Pankrats, G. A. Petrakovskii, M. A. Popov, K. A. Sablina, L. A. Prozorova, S. S. Sosin, G. Szimczak, R. Szimczak, and M. Baran, JETP Lett. **78**, 569 (2003).
7. Y. Kousaka, S. Yano, M. Nishi, K. Hirota, and J. Akimitsu, J. Phys. Chem. Solids **68**, 2170 (2007).
8. K. N. Boldyrev, R. V. Pisarev, L. N. Bezmaternykh, and M. N. Popova, Phys. Rev. Lett. **114**, 247210 (2015).
9. G. A. Petrakovskii, K. A. Sablina, D. A. Velikanov, A. M. Vorotynov, N. V. Volkov, and A. F. Bovina, Crystallogr. Rep. **45**, 853 (2000).
10. K. S. Aleksandrov, B. P. Sorokin, D. A. Glushkov, L. N. Bezmaternykh, S. I. Burkov, and S. V. Beluschenko, Phys. Solid State **45**, 41 (2003).
11. G. A. Petrakovskii, A. D. Balaev, and A. M. Vorotynov, Phys. Solid State **42**, 321 (2000).
12. G. Nénert, L. N. Bezmaternykh, A. N. Vasiliev, and T. T. M. Palstra, Phys. Rev. B **76**, 144401 (2007).
13. G. A. Petrakovskii, A. I. Pankrats, M. A. Popov, A. D. Balaev, D. A. Velikanov, A. M. Vorotynov, K. A. Sablina, B. Roessli, J. Schefer, A. Amato, U. Staub, M. Boehm, and B. Ouladdiaf, Low Temp. Phys. **28**, 606 (2002).
14. M. Fiebig, I. Sänger, and R. V. Pisarev, J. Appl. Phys. **93**, 6960 (2003).
15. A. I. Pankrats, G. A. Petrakovskii, L. N. Bezmaternykh, H. Szymczak, A. Nabialek, and B. Kundys, Phys. Solid State **48**, 330 (2006).
16. K. B. Vlasov, R. I. Zainullina, and M. A. Milyaev, Sov. Phys. JETP **72**, 169 (1991).
17. A. Pankrats, G. Petrakovskii, V. Tugarinov, K. Sablina, L. Bezmaternykh, R. Szymczak, M. Baran, B. Kundys, and A. Nabialek, J. Magn. Magn. Mater. **300**, e388 (2006).
18. P. M. Chaikin and T. C. Lubensky, *Principles of Condensed Matter Physics* (Cambridge Univ. Press, Cambridge, 1999).

Translated by K. Shakhlevich